Ultra-fast silicon detectors

H. F.-W. Sadrozinski [a,*], S. Ely [a], V. Fadeyev [a], Z. Galloway [a], J. Ngo [a], C. Parker [a], B. Petersen [a], A. Seiden [a], A. Zatserklyaniy [a], N. Cartiglia [b], F. Marchetto [b], M. Bruzzi [c], R. Mori [c], M. Scaringella [c], A. Vinattieri [c]

[a] Santa Cruz Institute for Particle Physics, UC Santa Cruz, Santa Cruz, CA 95064, USA
[b] INFN Torino, Torino, Italy
[c] University of Florence, Department of Physics and Astronomy, Sesto Fiorentino, Firenze, Italy

ARTICLE INFO

ABSTRACT

We propose to develop a fast, thin silicon sensor with gain capable to concurrently measure with high precision the space (~10 μm) and time (~10 ps) coordinates of a particle. This will open up new application of silicon detector systems in many fields. Our analysis of detector properties indicates that it is possible to improve the timing characteristics of silicon-based tracking sensors, which already have sufficient position resolution, to achieve four-dimensional high-precision measurements. The basic sensor characteristics and the expected performance are listed, the wide field of applications are mentioned and the required R&D topics are discussed.

1. Introduction

We propose an ultra-fast silicon detector (UFSD) which will establish a new paradigm for space-time particle tracking [1]. Presently, precise tracking devices determine time quite poorly while good timing devices are too large for accurate position measurement. This fact is imposing severe limitations on the potential of many applications ranging from medical PET to mass spectroscopy or particle tracking.

We plan to develop a single device able to concurrently measure with high precision the space (~10 μm) and time (~10 ps) coordinates of a particle. Our analysis of the properties of silicon pixel detectors (which already have sufficient position resolution) indicates that it is possible to improve their timing characteristics to achieve this goal. Since UFSD are extremely thin, they will make use of the internal charge multiplication in silicon sensors; a recent very active field of investigations within the CERN based RD50 collaboration [2].

In the following, we describe the principle of the UFSD, their properties and expected performance, followed by a section on measured pulse shapes. We present improvements in present applications and potential new applications with an UFSD system, and discuss required research.

2. Principle of UFSD

We propose to develop silicon sensors with time resolution a factor 100 better than what is possible today.

This proposal has to overcome a crucial limitation: given that the drift velocity in silicon saturates at about 10^7 cm/s, the collection time of electrons inside a silicon layer of ~300 μm is ~3 ns. Fast silicon sensors need therefore to be very thin and be able to function even though the charge collected is reduced with respect to that of thicker sensors. However, since the time resolution of a sensor depends on the signal-to-noise ratio, the charge collected from a thin active layer might not be enough to achieve good time resolution. We propose to exploit charge multiplication to increase the charge yield of very thin silicon sensors so that they can generate ultra-fast timing signals [1].

2.1. Gain in silicon sensors

The observation by several RD50 groups [2] of moderate gain in silicon sensors creates the opportunity for producing thin, very fast silicon sensors, which can work at extremely high-rates without dead-time issues. Up to now, the interest in moderate charge multiplication has been confined to mitigate charge collection loss due to trapping in irradiated sensors [3–6]. Our proposal is, instead, to make use of charge multiplication, with a gain of 10–100, to boost the small amount of charge collected in thin silicon sensors and to develop silicon sensors with ultra-fast timing information.

* Corresponding author. Tel.: +1 831 459 4670; fax: +1 831 459 5777.
E-mail address: hartmut@scipp.ucsc.edu (H.F.-W. Sadrozinski).

It has been demonstrated that in silicon sensors the charge multiplication factor α, which is responsible for the charge gain, has an exponential dependence on the electric field [7,8]. At the breakdown field in silicon sensors, $E_{max} = 270$ kV/cm, the maximum achievable multiplication is limited to about ~1/μm for electrons and ~0.1/μm for holes. N_0 electrons, drifting a distance d, with a charge multiplication factor α become N_{Tot} electrons:

$$N_{Tot} = N_0 e^{\alpha * d}$$

For example, one electron drifting 5 μm in a field $E_{max} = 270$ kV/cm with $\alpha = 0.746$ μm^{-1} from Ref. [7] generates a gain $g = N_{Tot}/N_0 = 42$. The effect of gain in silicon is similar to multiplication in gases employed in many detector applications and we can identify the parameter α with the first Townsend coefficient [9].

The electric field strength, however, is not a free parameter that can be set independently to obtain a high value of alpha, since it depends on the sensor bias. There is therefore interplay among biasing conditions, geometry and gain. To obtain the best possible timing performance, the charge collection time should be kept as short as possible. This requirement, combined with the saturation of the drift velocity, limits the region from which the charges can be collected to a thin volume close to the electrode (n^{++} implant in n-on-p sensors).

2.2. Effect of sensor thickness: electrical field, collected charge, collection time, and capacitances

To illustrate the problem, we consider a pad silicon sensor made by a single diode with a linear electric field and the bias voltage V_{bias} chosen so that the field at the p–n junction is at the maximum useful value, i.e. $E_{max} = 270$ kV/cm. For this configuration, Table 1 lists, as a function of the resistivity, for two choices of sensor thickness, the voltage to obtain full depletion (VFD), the applied bias voltage (bias), the minimum electric field E_{min} inside the sensor and the associated gain g.

The table shows two important facts: (i) the maximum gain is obtained when the bias voltage is much larger than the bias voltage needed for full depletion VFD: $V_{bias}/\text{VFD} \gg 1$ and (ii) throughout the entire sensor bulk the electrons are moving at the highest possible velocity since the field exceeds everywhere 20 kV/cm, the field required for saturating the drift velocity [10].

The thickness of the active area determines several key parameters of the sensor. Considering two possible geometries, (i) a 50 μm × 50 μm pixel and (ii) a 1 mm-long strip ("striplet") with 50 μm pitch, Table 2 shows, as a function of sensor thickness, the backplane capacitance, the number of electrons that form the signal, the collection time, and the gain required to reach an acceptable signal level, 2000 electrons for the pixel, and 12,000 electrons for the strip sensor. The expected signal before gain is taken from Ref. [11].

Table 1
Voltage of full depletion VFD, bias voltage, minimum electric field and gain for silicon sensors of two different thicknesses and various resistivity values with the condition that the maximum electric field is $E_{max} = 270$ kV/cm.

Resistivity [kΩ-cm]	Thickness [um]							
	20				5			
	VFD [V]	Bias [V]	E_{min} [kV/cm]	Gain	VFD [V]	Bias [V]	E_{min} [kV/cm]	Gain
0.01	453				28	107	157	3.0
0.02	227	314	44	19	14	121	214	4.9
0.1	45	495	225	4.9×10^3	2.8	132	258	9.1
1	4.5	535	265	1.7×10^5	0.28	135	268	10.9
10	0.45	540	270	2.9×10^5	0.028	135	270	11.3

Table 2
Silicon sensor characteristics for various thicknesses of the active area.

Thickness [μm]	Back-plane capacitance		Signal [# of e$^-$]	Collection time [ps]	Gain required	
	Pixels [fF]	Strips [pF/mm]			For 2000 e$^-$	For 12000 e$^-$
1	250	5.0	35	13	57	343
2	125	2.5	80	25	25	149
5	50	1.0	235	63	8.5	51
10	25	0.50	523	125	3.8	23
20	13	0.25	1149	250	1.7	10.4
100	3	0.05	6954	1250	0.29	1.7
300	1	0.02	23334	3750	0.09	0.5

Thinning sensors increases the back-plane capacitance. If one requires noise performance of thin sensors to be comparable to thick ones, one would limit the back-plane capacitance to be not much larger than the interstrip capacitance (200 fF for existing pixel sensors and 1 pF/cm for n-on-p strip sensors). This limits the thickness of pixel sensors to be larger than 1 μm and one of the strip sensors to be larger than 20 μm.

From the values shown in Table 2, pixel sensors offer very attractive combinations of moderate gain, small capacitance, and short collection time. Up to now, a gain of 6.5 has been reported in studies with epitaxial pad sensors [6]: this fact makes us confident that with a full research program we can achieve higher gains. Due to the high value of backplane capacitance, strip sensors cannot be made as fast as pixel sensors; however, a 1 mm long and 5 μm thick "mini-strip" offers a quite fast collection time, 50–100 ps, with a moderate value of capacitance (~1 pF).

3. Properties of thin segmented sensors

3.1. Sensor options: epitaxial and thinned float zone

A key part of the project is the possibility to mold the design of UFSD to the needs of different fields. For example, in medical applications such as PET, the sensor can be adapted, via backside etching, to detect visible light while in charge particles detection this is not necessary. Likewise, in applications such as x-ray crystallography at energies below 5 keV and sensors of ~20 um thickness. or dose counting the read-out chip can be designed, due to the very fast input pulse, to have unmatched single particle counting capabilities, while in time-of-flight experiments the fast input pulse is exploited to reduce the uncertainty on the time of arrival.

Thin epitaxial sensors are easily produced since they consist of a low-resistivity electrode (n^{++}) implanted in a high-resistivity p-epitaxial layer of silicon, deposited on a thick low-resistivity p^{++} substrate and the read-out chip is bump bonded to the sensor, Fig. 1a. In this configuration, they are very efficient in detecting charged particles. However, this configuration does not allow the detection of visible photons since the sensitive epi-layer is sandwiched between two fairly thick low-resistivity layers, the substrate and the ASIC.

As the detection of visible photons is one of the main fields of application of UFSD (for example PET and robotic vision), we foresee to employ backlit thinned high-resistivity Float Zone (FZ) sensor, Fig. 1b. In this technique one processes a FZ wafer of normal thickness and removes the excessive material at the backside by etching. Several groups have produced back-etched thin sensors [12–14], down to 15 μm thickness. In particular we propose to adapt a backside thinning method using a selective
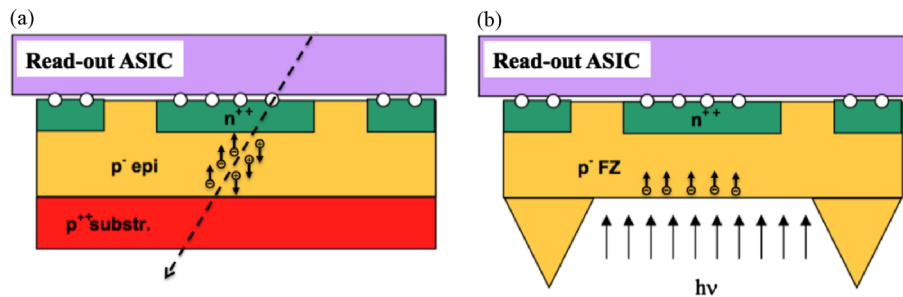
Fig. 1. UFSD sensor bump bonded to a read-out ASIC (not to scale); (a) sketch of an epitaxial sensor for detection of charged particles; (b) sketch of a back-thinned FZ sensor for detection of photons (including ribs to improve mechanical rigidity).

etch to create ribs for mechanical strength. Given the low costs and quick manufacturing turn-around time, thin epitaxial sensors are an ideal low-cost vehicle for prototyping, e.g. for optimizing the field configuration and other key parameters, before producing thinned sensors.

3.2. Tuning of the electric field

As mentioned above, our concept is based on the idea of using moderate gain ($g < 1\,0\,0$) and to bias the sensors below the breakdown voltage. This sets us apart from the related field of silicon photomultipliers, yet allows us to tap into the very active development effort of avalanche based sensors, where the electric field is tuned by implants and deep diffusion [15,16].

Up to now, charge multiplication has been mainly observed in sensors irradiated with hadronic fluences beyond 10^{15} neutron equivalent/cm^2, with a possible observation in highly over-depleted n-type 3D sensors [5]. The reason for this fact is that irradiated sensors operate at a field high enough to have charge multiplication while non-irradiated sensors tend to exhibit electrical breakdown before reaching the required high fields. One goal of our project is to design a sensor with a geometry and doping profile that achieves charge multiplication without having electrical breakdown.

Without careful design of the doping profile, charge multiplication happens only in small areas of the sensor, for example near the strip edges where the field lines become very dense. However, to achieve charge multiplication across a much larger volume, the bias voltage needs to be increased to such high values that it causes electrical breakdown at the strip edges. It is therefore necessary to change the geometry of the field lines inside a sensor in order to prevent this problem, while achieving a large enough volume with high field.

This idea can be accomplished by introducing two major changes to the traditional implant profile of planar segmented sensors: (i) increase the width and the depth of the n^{++} implant in order to reduce the large fields that are present at its edges and (ii) diffuse just below the n^{++} implant a p$^+$ layer to create a large n^{++}-p$^+$- p- junction along the center of the electrodes [17]. Under reverse bias conditions, a high electric field region is created in this localized region. By tailoring the depth and/or doping concentration of the additional p$^+$ diffusion layer, it is possible to adjust the maximum electrical field across the strip width, which can lead to approximately equal multiplication mechanism across the electrode.

4. Measurements of pulse shapes in thin un-irradiated pad sensors

We expect the pulse shapes in charge collection studies to reveal details of the charge collection dynamics. For this we used
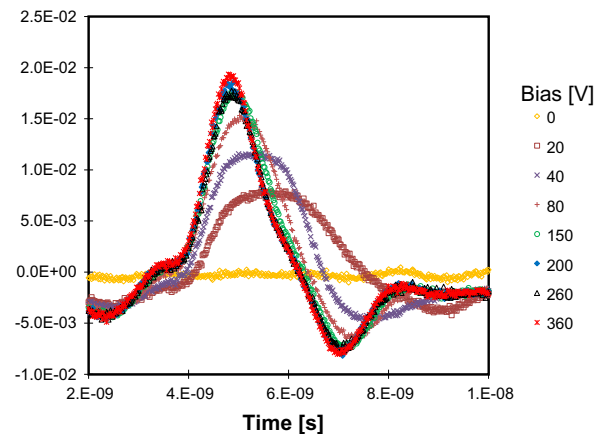
Fig. 2. Response of the high-resistivity thinned FZ pad sensor to impulses from a picosecond 730 nm (red) laser: averaged pulse shapes for different bias voltages. (For interpretation of the references to color in this figure legend, the reader is referred to the web version of this article.)

existing pad sensors of 50 μm thickness of either high-resistivity n-type bulk [13] or low-resistivity p-type epi sensors [18]. Using a picosecond (ps) lasers to generate the charges in the bulk provides the advantage of reduced noise afforded by averaging many almost identical pulses, while α particles provide a large signal in a limited sensor depth. In the following we show the charge collection data using the red laser only, since the data with α particles are very similar. The results did not show charge multiplication, as expected, and the rise times were limited by the bandwidth of the oscilloscopes used.

The thinned p-on-n FZ sensors used are described in [13]. With C–V measurements, their thickness was confirmed to be 50 μm and the resistivity to be 6 kΩ-cm, with a depletion voltage of ~1–2 V. A beam from a mode-locked ps Ti:Sapphire laser (manufacturer: Tsunami-Spectra Physics), tuned at 740 nm and producing 1.2 ps pulses with a repetition rate of 81.3 MHz was focused on the sensor to form a spot of approximately 100 μm diameter, being absorbed in approximately 6 μm depth. The signal was read-out by an oscilloscope with 500 MHz bandwidth and 50 Ω input impedance.

The recorded pulse averages shown in Fig. 2 saturate between 80 and 150 V bias. The maximum E-field observed at 360 V is about 75 kV/cm, much below the value where charge multiplication is expected. Pulse distortions are caused by the rapid succession of the pulses and the non-optimized signal transmission, and the observed baseline shift is due to AC coupling. The pulses are a convolution of electronic shaping and charge collection time structure, which is due to holes being collected in a short time and to electrons drifting away from the implant. We fit the pulses to a RC-CR function to determine the shaping rise time ("trise") and the actual 10–90% rise rime ("RT10-90"). In addition we determine
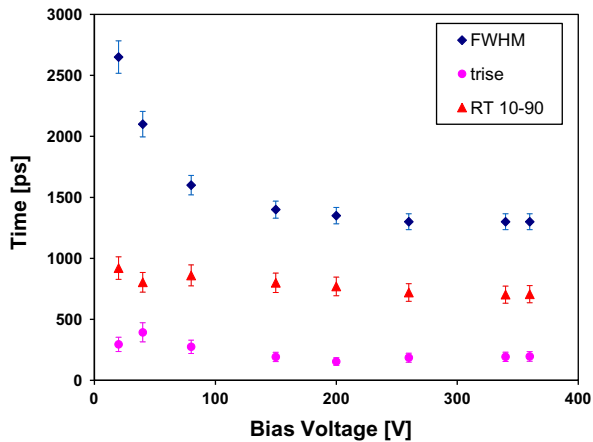
Fig. 3. Response of the high-resistivity thinned FZ pad sensor to impulses from a picosecond 730 nm (red) laser: bias voltage dependence of three pulse time parameters: pulse width ("FWHM"), shaping rise time ("trise"), and 10–90% rise time ("RT10-90"). (For interpretation of the references to color in this figure legend, the reader is referred to the web version of this article.)

the FWHM width for the pulses, which represents best the convolution mentioned above. These three are plotted in Fig. 3 vs. the bias voltage. Both RT10-90 and trise are almost independent of bias within the error bars, showing that they are given by the bandwidth of the system. The FWHM pulse width levels off at about 150 V bias, indicating that the collection time becomes constant. This is due to the fact that at high electric field, i.e. $E > 25$ kV/cm, the drift velocity reaches a terminal value of ~100 μm/ns, i.e. a lowest collection time of ~500 ps. This field is reached at a bias voltage of 120 V, consistent with our observation. Below 120 V bias, the unsaturated drift velocity increases the charge collection time, causing the pulses to widen.

5. Applications of UFSD

The development of UFSD research is poised to open up a range of new opportunities for applications that benefit from the combination of position and timing information. For example, UFSD allows obtaining sharper PET images, monitoring more accurately the dose delivered in cancer treatment and improving particle tracking in High-Energy physics experiments.

The combined spatial and timing precision offered by UFSD will represent a breakthrough and will enable applications in a whole array of different fields.

a) *Tracking*: Identifying with high precision the temporal signature of different events allows for their association and reduces random coincidences. Traditional tracking is often overwhelmed by combinatorial backgrounds, which can be drastically reduced by adding a 4th dimension per point.

b) *Time of Flight* (ToF): ToF is already used in many commercial applications such as ToF-enhanced PET and mass spectroscopy ToF, however with precision more than one order of magnitude worse than the goal of UFSD (~500 ps vs. ~10 ps). ToF is also used in particle physics as a tool for particle identification.

c) *3D and Robotic Vision*: The ability to accurately measure the travel time of light pulses reflected by an object at unknown distance is of paramount importance to reconstruct 3D images, fundamental in imaging and robotic vision. UFSD will offer a spatial precision of a few millimeters, revolutionizing the current applications.

d) *Particle counting*: UFSD performance would allow developing new tools in single particle counting applications with

unprecedented rate capabilities. For example, in the treatment of cancer using hadron beams, such a tool would measure the delivered dose to patients by directly counting the number of hadrons. Material science experiments using soft x-rays will benefit from the combination of high rate and precision location that UFSD offers.

We outline here more details on two relevant applications.

5.1. Time of flight for particle identification in space

In space sciences, there is a great interest in identifying the type of charged particles measured. For example, the Alpha Magnetic Spectrometer (AMS) detector [19], operating on board of the International Space Station ISS since 2011, performs precision measurements of cosmic ray composition and flux. The momentum of the particles is measured with high-resolution silicon sensors inside a magnetic field of about 1 m length. Instrumenting UFSD within the magnet, with a time resolution of 10 ps, would allow reaching the "Holy Grail" of Cosmic Ray Physics: the distinction between anti-carbon ions and anti-protons up to a momentum of 200 GeV/c.

5.2. Time of flight for Positron Emission Tomography PET

Positron Emission Tomography (PET) is the most powerful and extensive system to probe the human physiology. It is also a diagnostic tool used to detect physiological modifications in tissues. Cancer prevention calls for early detection of such changes, which strongly depends on the spatial resolution [20].

The fact that the position resolution of the UFSD system will be more than a factor 10 better than that of a PET system using very fast silicon photomultipliers (SiPM) [21] yet with comparable time resolution is one of the motivations for the development of UFSD.

A key factor to improve the time resolution relies on the possibility to reduce the background present in the measurement. The frequency of accidental almost-back-to-back photons, which mimics a genuine electron–positron annihilation followed by two 511 keV photons at 180°, is directly related to the time window within which the photons are considered as emitted by the same process. By substantially increasing the precision on the arrival time of the photons, one can tighten the window thus reducing the number of spurious events.

Commercial PET systems have time resolutions somewhat less than 1 ns [22], which, considering the speed of light, corresponds to a 30 cm uncertainty in the position of the annihilation along the line-of-view: with UFSD we aim at decreasing this number by an amount close to two orders of magnitude. Since the signal-to-noise ratio in PET images scales linearly with the time resolution, this reduction will considerably enhance the image quality and or reduce the dose to the patient. The other, more important, issue is the possibility to detect even small physiological changes mainly related to early cancer lesions as the signal-to-noise ratio increases.

6. Research issues

In the sections above, we have outlined our idea for a thin silicon sensor with built-in charge multiplication using what we think is the most promising solution: planar n-on-p silicon sensor. However there are several other choices that might be explored and can lead to our goals.

6.1. Wafer type: p-on-n and n-on-p

Several arguments seem to favor n-on-p sensors (which collect electrons) over p-on-n (which collect holes): the collection of electrons is faster, electrons have a factor of 10 larger multiplication gain than holes [7,8] and there have been many studies on radiation-hardness of p-type sensors for the LHC upgrade [23–25]. But at saturation the drift velocities of electrons and holes are almost equal, and charge multiplication has been observed from both electrons drifting towards the electrode (like in p-type sensors) and drifting away from the electrons (like in n-type sensors), respectively [5,6].

6.2. Planar and 3D

Planar sensors collect charges in implants on the surface, while 3D sensors [26] collect charges in columns implanted in the sensor bulk. For 3D sensors, there are good theoretical arguments [27] and data [5] supporting their use as fast sensors with gain, but the possible drawback such as low-field regions and the need to synchronize the particle entry time might limit their usefulness.

6.3. Simulations

An important research activity will be the optimization of the electrical field. Our project involves efforts to both better quantify what is physically happening in the sensor and to tailor the field to optimize the performance for timing purposes and for minimum material. The gain phenomenon in segmented silicon sensors is in need of deeper understanding, in part due to the difficulty of modeling non-uniform electrical field near the collecting electrode [17,28,29]. Other important issues are: (i) over-depletion and breakdown in sensors on p-type and n-type wafers, (ii) field shaping at the n^{++} implant edge with deep diffusion, (iii) field shaping underneath the n^{++} implant with selective p^+ implant, (iv) thinning of the backside of the sensor, and (v) generation of "slim" edges to permit seamless tiling [30].

6.4. Readout electronics

Because of the very demanding requirements for the time measurement in the UFSD system, an ASIC solution is the natural choice for the read-out electronics. Such a solution will benefit from the performances of the most advanced technologies both in terms of circuit density (for space resolution) and of circuit speed (for time resolution). The research activity on the ASIC design will have to analyze and decide on a number of important issues, in terms of both architecture, e.g. constant fraction discriminator (CFD) vs. amplitude correction, Time-to-Analog Converter (TAC) vs. Delay-Locked Loop (DLL) and technologies (CMOS vs. SiGe). An encouraging fact is that the work for the NA62 Gigatracker has resulted already in a pixel readout ASIC with 100 ps time resolution [31,32].

7. Conclusions

We are proposing the development of a "4-dimensional" tracker using thin ultra-fast segmented silicon detectors with position resolutions of 10's of micrometers and a fast readout to reach time resolution of 10's of picoseconds, based on moderate internal gain. The list of applications benefiting from the UFSD is long.

Considerations of capacitances and signal collection constrain feasibility to sensor thickness of about 5 μm for pixels and about 20 μm for short strip. A few topics for crucial simulations and for sensor development have been identified. The most important task is to even out the gain in segmented sensors and to allow large over-depletion without breakdown.

Acknowledgments

References

[1] H.F.-W. Sadrozinski, Exploring charge multiplication for fast timing with silicon sensors, in: Proceedings of the 20th RD50 Workshop, Bari, Italy, May 30–June 1, 2012, ⟨https://indico.cern.ch/conferenceOtherViews.py?view=standard&confId=175330⟩.

[2] RD50 Collaboration, ⟨http://rd50.web.cern.ch/rd50/⟩.

[3] I. Mandic, et al., Study of anomalous charge collection efficiency in heavily irradiated silicon strip detectors, Nuclear Instruments and Methods A 636 (2011) 50–55.

[4] G. Casse, et al., Enhanced efficiency of segmented silicon detectors of different thicknesses after proton irradiations up to 1×1016 neq cm^2, Nuclear Instruments and Methods A 624 (2) (2010) 401–404.

[5] M. Köhler, et al., Comparative studies of irradiated 3D silicon strip detectors on p-type and n-type substrate, in: Proceedings of the 17th RD50 Workshop CERN Switzerland, 17–19 November, 2010, ⟨http://indico.cern.ch/getFile.py/access?contribId=4&sessionId=4&resId=0&materialId=slides&confId=111191⟩.

[6] J. Lange, et al., Properties of a radiation-induced charge multiplication region in epitaxial silicon diodes, Nuclear Instruments and Methods A 622 (2010) 49–58.

[7] W. Maes, K. De Meyer, R. Van Overstraeten, Impact ionization in silicon, a review and update, Solid-State Electronics 33 (6) (1990) 705–718.

[8] A. Macchiolo, Impact ionization in silicon detectors, in: Proceedings of the16th RD50 Workshop Barcelona, Spain, 2010, ⟨http://indico.cern.ch/getFile.py/access?contribId=3&sessionId=3&resId=0&materialId=slides&confId=86625⟩.

[9] J.S. Townsend, Electricity in Gases, Clarendon Press, Oxford, 1915.

[10] G. Kramberger, et al., Electric field and space charge in neutron irradiated n^+-p sensors, in: Proceedings of the 19th RD50 Workshop CERN, Switzerland, Nov 21–23, 2011, ⟨http://indico.cern.ch/getFile.py/access?contribId=7&sessionId=1&resId=0&materialId=slides&confId=148833⟩.

[11] S. Meroli, D. Passeri, L. Servoli, Energy loss measurement for charged particles invery thin silicon layers, in: Proceedings of the 11 JINST 6 P06013, 2011.

[12] M. Lozano, IMB-CNM Radiation Detectors Activities, AIDA Project Kick-off Meeting, CERN, Feb 2011, ⟨http://indico.cern.ch/conferenceDisplay.py?confId=125221⟩.

[13] M. Beimforde, et al., First characterizations of thin SOI and epitaxial n-in-p sensors, in: Proceedings of the 14th RD50 Workshop, Freiburg, Germany, 2009, ⟨http://indico.cern.ch/conferenceOtherViews.py?view=cdsagenda&confId=52883⟩.

[14] G.-F. Dalla Betta, et al., High-performance PIN photodiodes on TMAH thinned silicon wafers, Microelectronics Journal 39 (2008) 1485–1490.

[15] C. Piemonte, A new silicon photomultiplier structure for blue light detection, Nuclear Instruments and Methods A 568 (2006) 224.

[16] T. Nagano et al., Timing Resolution Improvement of MPPC for TOF-PET Imaging, in: Proceedings of the 2012 IEEE NSS-MIC, Anaheim, CA, Oct 29–Nov 3, 2012.

[17] P. Fernandez, et al., Simulation of new p-type strip detectors with trench to enhance the charge multiplication effect in the n-type electrodes, Nuclear Instruments and Methods A 658 (2011) 98–102.

[18] M. Bruzzi, M. Bucciolini, M. Casati, D. Menichelli, C. Talamonti, C. Piemonte, B. G. Svensson, Epitaxial silicon devices for dosimetry applications, Applied Physics Letters 90 (2007) 172109.

[19] ⟨http://www.nasa.gov/mission_pages/station/research/experiments/AMS-02.html⟩.

[20] V.Ch. Spanoudaki, C.S. Levin, Photo-detectors for time of flight positron emission tomography (ToF-PET), Sensors 10 (2010) 10484–10505.

[21] S.J. Hong, et al., SiPM-PET with a short optical fiber bundle for simultaneous PET-MR imaging, Physics in Medicine and Biology 57 (2012) 3869–3883.

[22] Siemens, Improving PET With HD•PET+Time of Flight, ⟨www.siemens.com/mi⟩.

[23] M. Bruzzi, H.F.W. Sadrozinski, A. Seiden, Comparing radiation tolerant materials and devices for ultra rad-hard tracking detectors, Nuclear Instruments and Methods A 579 (2007) 754–761.

[24] Y. Unno, et al., Development of n-on-p silicon sensors for very high radiation environments, Nuclear Instruments and Methods A 636 (2011) 24–30.

[25] A. Affolder, et al., Silicon detectors for the sLHC, Nuclear Instruments and Methods A 658 (2011) 11–16.

[26] S.I. Parker, C.J. Kenney, J. Segal, 3D-A proposed new architecture for solid state radiation detectors, Nuclear Instruments and Methods A 395 (1997) 328–343.

[27] S. Parker, et al., Increased speed: 3D silicon sensors; fast current amplifiers, IEEE Trans. Nucl. Sci. NS-58 (2011) 404.

[28] E. Verbitskaya, Operational conditions for enhancement of collected charge via avalanche multiplication in n-on-p strip detectors, in: Proceedings of the 20th RD50 Workshop Bari, Italy, May 2012, ⟨https://indico.cern.ch/getFile.py/access?contribId=0&sessionId=4&resId=0&materialId=slides&confId=175330⟩.

[29] M. Benoit, et al., Simulation of charge multiplication and trap-assisted tunnelling in irradiated planar pixel sensors, in: Proceedings of the IEEE Nuclear Science Symposium and Medical Imaging Conference, October2010, pp. 612–616.

[30] M. Christophersen, et al., Alumina and silicon oxide/nitride sidewall passivation for P- and N-type sensors, Nuclear Instruments and Methods A 699 (2013) 14–17.

[31] G. Dellacasa, S. Garbolino, E. Marchetto, S. Martoiu, G. Mazza, A. Rivetti, R. Wheadon, A silicon pixel read-out ASIC with 100 ps time resolution for the NA62 experiment, in: Proceedings of the JINST 6 C01087, 2011.

[32] L. Perktold et al., A 9-Channel, 100 ps LSB time-to-digital converter for the NA62 gigatracker read-out ASIC (TDCpix), In Proceedings of the JINST 7 C01065, 2012.